An Experimental and Analytical Approach to the Development of a Range of Neurovascular Trauma Indices

Robert J. Boock and Lawrence E. Thibault

Department of Bioengineering, University of Pennsylvania
114 Hayden Hall, Philadelphia, PA 19104, USA

ABSTRACT

Results from isolated blood vessel studies show a graded physiologic response to a mechanical stretch injury. The measured response shows a developed force post injury ranging from 2 to 7 grams. This corresponds to a decrease in diameter of approximately 7-12%.

An appropriately scaled materials testing device has been developed. This device consists of a solenoid driver, an isometric force transducer, an angular displacement transducer, as well as a fluid reservoir system.

A series of experiments involving dynamic elongation of fluid and air filled elastic tubes have been conducted together with the specimens of viable blood vessels. The polymer tube physical model allows us to more closely study the coupled fluid and solid mechanics problem associated with cerebral blood vessels undergoing high strain rate loading. These strains are comparable to those associated with traumatic head injuries. Comparisons between fluid and air filled elastic tubes show increased force measurements ranging from 10 to 43%. Using both physical and analytical models we can investigate the thresholds for a vasoreactive response (below the threshold for structural failure) elicited by mechanical loading of the head. It is felt that this response is elicited during impact and leads to a vasospasm; the concomitant decrease in cerebral blood flow can exacerbate the neural injury sustained.

INTRODUCTION

This report will focus upon the development of injury criteria for isolated blood vessels undergoing dynamic elongation. The emphasis is placed upon the functional response of the blood vessels (vasoreactivity) when subjected to high strain rate extension. Although the structural failure of neurovascular elements is of obvious importance, we believe that strain induced changes in cerebral blood flow due to vessel spasm, for example, can affect brain injury severity through hypoxic and ischemic effects which may amplify the severity of other diffuse brain injuries. Diffuse brain injury outcome may be seriously affected by the reduction of blood flow and the subsequent lack of oxygen metabolism and the effect on the cellular recuperative functions.

Gennarelli and Thibault [8] observed increases in intracranial pressure (ICP) immediately following acceleration of the head in experiments that reproduced diffuse axonal injury (DAI) and coma in primates. The animals, whose heads were accelerated laterally to produce these diffuse injuries, showed a sharp increase in intracranial pressure which then peaked and decayed exponentially with a 20-30 minute time constant (Figure 1).

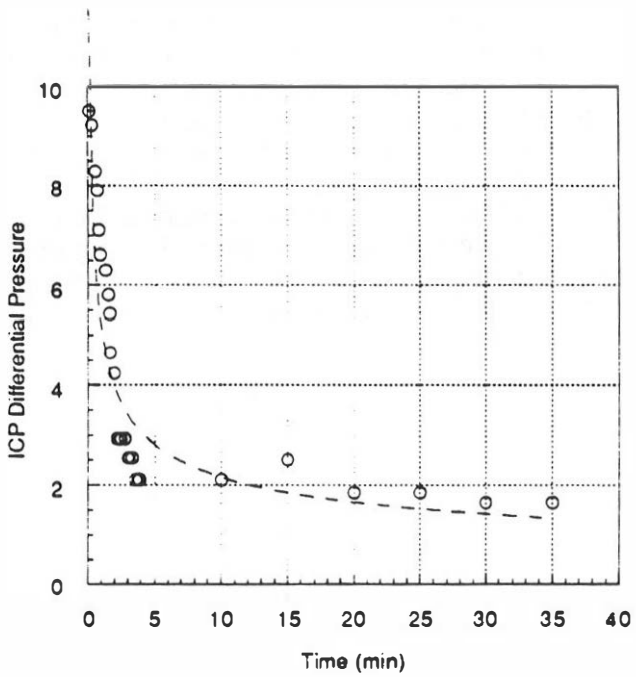

Figure 1 Change in ICP versus Time
ICP Differential Pressure = $(ICP_{post} - ICP_{trauma}) / (ICP_{baseline})$

Increases in ICP have not been observed clinically as the result of inertial injuries due to the short time course of the event; the peak intracranial pressure occuring within ten minutes of the traumatic insult. However, these rises in ICP have been corroborated utilizing the piglet fluid percussion model in which not only increases in ICP but also decreases in cerebral blood flow coupled with increases in cerebral vascular resistance were measured [22]. Blood flow studies were also performed in the guinea pig optic nerve model of DAI. In these studies, a decrease in blood flow was measured using a laser-doppler blood velocity probe during uni-axial, high strain rate extension of the optic neurovascular bundle [9]. In addition, clinical

observations of vasospasm [21] have been made in response to mechanical manipulation of vessels during neurosurgery.

We hypothesize that the change in ICP following inertial head injury is related to a transient decrease in intracranial circulation. Since this phenomenon is a nearly immediate response to the mechanical insult, edema and CSF shunting are not likely significant etiologic factors. Rather, we propose that inertial loading of the brain results in arterial dilation with concomittant venous spasm resulting in engorgement of cerebral circulation. This phenomenon is measured clinically as an increase in ICP.

In this research we reproduced the vascular response to mechanical loading in vitro utilizing isolated vessels. In vitro experiments minimize the complexity of the in vivo system in which chemical and electrical stimuli confound the mechanical loading condition. In addition, in vitro studies allow for the precise measurement of the mechanical stimulus experienced by the vessel under study due to the elimination of complex vessel orientation and brain geometry seen in vivo. The range of magnitudes of strain used were comparable to those experienced by the brain macroscopically [19]. We observed a continuum of physiologic response - from the reversible spasm to ultimate structural failure - in response to increasing levels of mechanical strain. This leads us to the possibility that an injury scale, similar to that for neural injury in DAI, may exist for blood vessels as well.

SYSTEM DESCRIPTION

A small-scale materials testing device has been developed. This apparatus is illustrated in Figure 2.

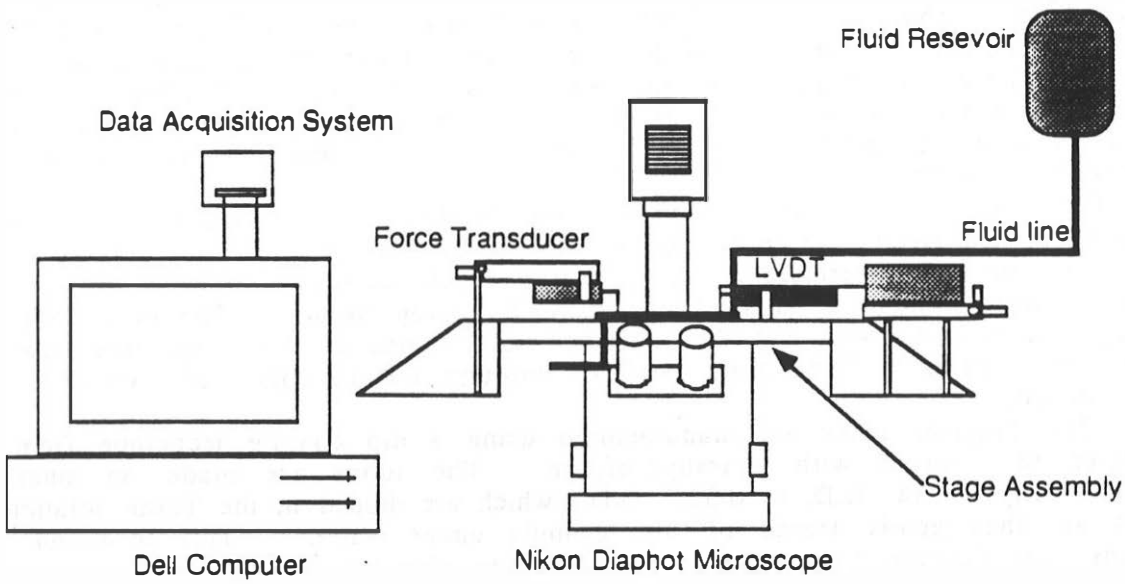

Figure 2 System Overview

The device consists of a solenoid driver, an isometric force transducer , a linear variable displacement transducer, as well as a fluid perfusion system. Details are given in Figure 3. This device has been designed to produce high strain rate deformations in the specimens to simulate the deformations seen in traumatic injuries. The materials testing platform will be centered upon a Nikon Diaphot inverted microscope. The microscope will serve as a platform for micromanipulators, measurement systems, and the mechanical driver for producing loads on the specimens. The microscope itself was modified to allow a Wild dissecting microscope to be attached in such a way that the vessel may be easily mounted. In addition to normal optical studies a Cohu CCD video camera and recorder will be attached directly

to the microscope to visually record the experimental event for qualitative and quantitative analysis of deformations.

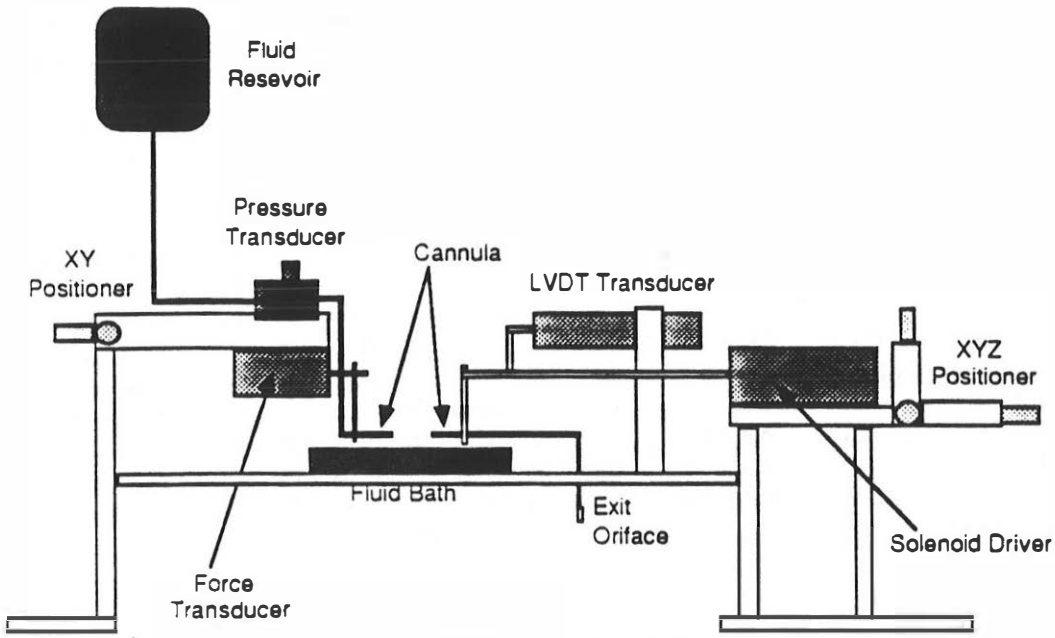

Figure 3 System Detail

Mechanical loading of the blood vessels will be accomplished by a solenoid attached to a chuck. This solenoid is a Ledux model 189711-025 and has been positioned parallel to the axis of loading. The velocity of specimen loading can be controlled from 40 to 120 cm/s through a change in loading voltage. Incorporated into this system is Trans-Tek 0217-0000 linear variable displacement transducer which is mounted parallel to the drive shaft of the solenoid for measurement of the displacement of the shaft .

Either the blood vessel or polymer tubes are directly attached over a cannula. This cannula is then attached to a chuck to allow access into the inner portion of the blood vessel or tube for perfusion. This entire chuck assembly attaches rigidly to the solenoid driver which is mounted on an XYZ micropositioner. The other side of the vessel is also cannulated and then attached to a chuck on the force transducer which allows the vessel to have fluid perfused through the cannula and controlled via an exit orifice.

The polymer tubes are manufactured using a dip coating technique from Texan polymer in solution with Tetrahydrofuran. The tubes are made on small glass cannula (range 0.018" O.D. to 0.025" O.D.) which are dipped in the Texan solution. The tubes are then gently teased off the cannula under water. This technique of dip coating was developed to easily manipulate the physical properties through a change in wall thickness and to be within the ranges for blood vessels of the same diameter.

The blood vessel specimens need to be immersed in an oxygenated Ringers solution in order to maintain viability. This is done by the fluid resevoir system. The Ringers solution was circulated and the temperature controlled. The solution is oxygenated by means of a gas bubbler connected to a gas cylinder (95% O_2 5% CO_2) which allows oxygen to be bubbled through these containers before the solution leaves the feed system. The pressure head was chosen to deliver 4 ml/min for perfusion to maintain vessel viability. In addition, a PiTran model PT-L2-M03 pressure transducer will be incorporated into the feed system to measure the pressure transients over the vessel and thus provide a quantitative determination of response.

The data acquisition system is based on a Dell 310 PC/AT compatible computer system. Analog signal conditioning and interfacing was accomplished by an

Metrabyte DAS-16F high speed analog and digital board with 16 input channels and 2 output channels.

RESULTS AND DISCUSSION

Viable blood vessels obtained from the rat were dynamically stretched using our custom small scale material testing platform. Force and displacement were measured in real time in response to impulse loading conditions at several levels of ultimate strain and a strain rate of 24 sec^{-1}. Post-injury developed force and luminal cross-sectional area were measured immediately following mechanical insult. Figure 4 illustrates the developed force time histories for five vessels loaded to different levels of ultimate strain of physiologic importance [14]. For 6% ultimate strain occuring at time 0, force develops in one vessel beginning at 15 seconds, plateaus at a peak force of 1.7 grams at 50 seconds, and then, beginning at 80 seconds returns to baseline which is reached at 120 seconds. In the second specimen stretched to an 8% ultimate strain, force develops beginning at 20 seconds, plateaus at a peak force of 2 grams at 50 seconds, and then, beginning at 85 seconds returns to baseline which is reached at 110 seconds. In the third specimen stretched to an 9% ultimate strain, force develops beginning at 30 seconds, reaches a peak force of 3.2 grams at 55 seconds, and then, beginning at 60 seconds returns to baseline which is reached at 105 seconds. In the fourth specimen stretched to an ultimate strain of 11%, post-injury force develops at 35 seconds, reaches a peak of 3.8 grams at 55 seconds, plateaus at this level until 80 seconds, and then returns to baseline by 130 seconds. In the fifth specimen stretched to an ultimate strain of 15%, post-injury force develops at 20 seconds, reaches a peak of 6.8 grams at 90 seconds, and then returns to baseline by 120 seconds. The only vessels to react to the this mechanical stimulus have been the veins, although equal numbers of arteries were tested. We hypothesize that equivalent loads applied to the arteries result in lower stress in the walls and thus lower strains in the cells that will react to this stimulus (vascular smooth muscle). Another possibility is the fact that the arteries may be more able to recover from this injury because of their ability to continiously adapt to control blood flow.

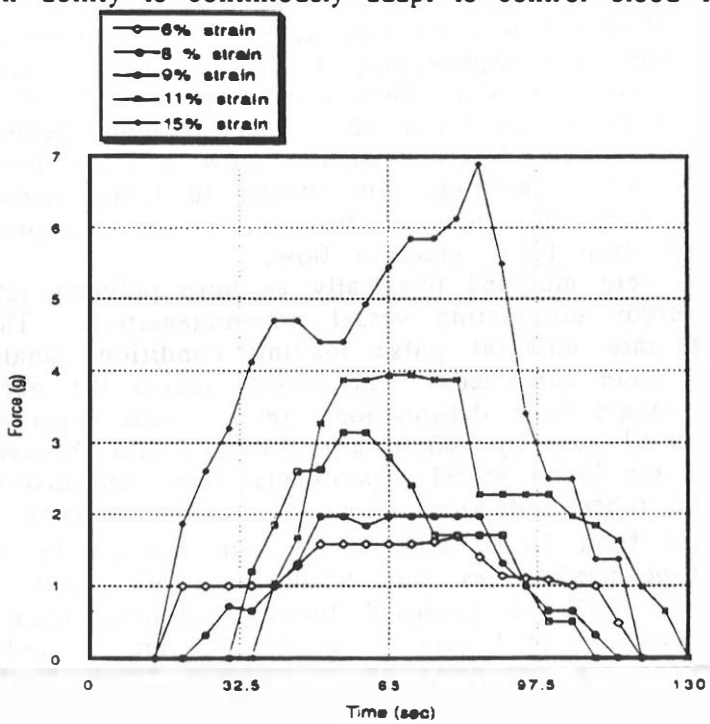

Figure 4 Developed Force versus Time for Viable Blood Vessels (Post -stretch)

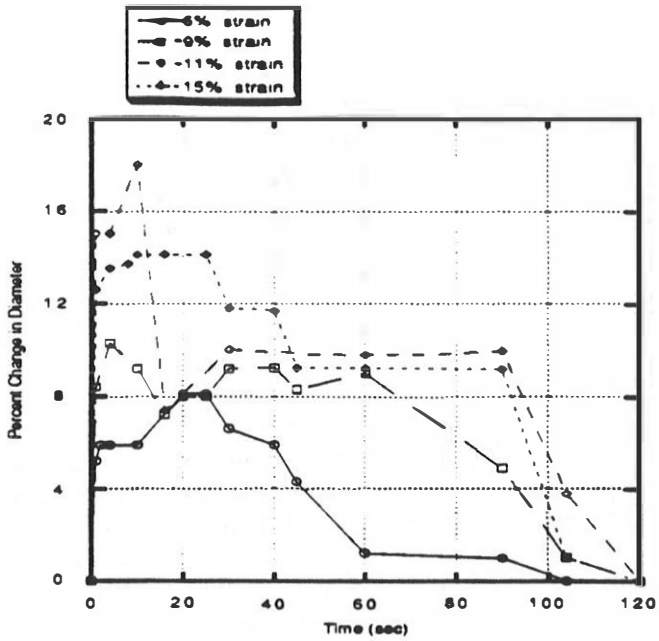

Figure 5 Measurement of Diameter change for Viable Blood Vessels (Post-stretch)

Quantitative video microscopy was used to measure post-injury luminal diameters. For the specimen experiencing an 6% ultimate strain, an immediate 6% decrease in luminal diameter was followed by a peak decrease in luminal diameter of 8% within 20 seconds of the insult (see Figure 5). The specimen experiencing an 9% ultimate strain, an immediate 10% decrease in luminal diameter was followed by a relative plateau in luminal diameter of 9% within 15 seconds of the insult. For the specimen experiencing an 11% ultimate strain, an immediate 16% decrease in luminal diameter was followed by a peak decrease in luminal diameter of 18% within 10 seconds of the insult, which then plateaued at a decrease of 10% and then returned to baseline at 120 seconds. For the specimen experiencing an 15% ultimate strain, an immediate 12% decrease in luminal diameter was followed by a peak decrease in luminal diameter of 14% within 15 seconds of the insult which then gradually returned to baseline at 120 seconds. Assuming simple Hagen-Poiseuille flow and an average lumen change of approxiamtely 10% for 2 minutes, this change in lumen cross-sectional area would result in either a 40% reduction of flow for a constant pressure drop or a 40% increase in pressure drop for a constant flow.

Blood vessels were modeled physically as pure polymer tubes synthesized out of Texan polymer thereby eliminating vessel inhomogeneities. These tubes were tested under high strain rate uniaxial pulse loading conditions analagous to those under which the vessels were subjected. The results reveal the nonlinear elastic response of the tubes to a single large deformation stretch. This experiment was then extended to a more complicated case by adding a perfusing liquid through this polymer tube.

Analagous to the blood vessel experiments, force and displacement were measured in real-time as the tubes underwent impulse uniaxial extension in a range of strains. For ultimate strains from 10 to 50% at a strain rate of 18 sec^{-1}, the peak force developed in non-perfused tubes was from 5 to 50 grams. This developed force increased by 10 to 43% in perfused tubes depending upon variabilities in wall thickness of the tubes. In Figure 6 the results from a single experimental set are shown as the forces are converted to an average longitudinal stress (12 percent difference) and the data is limited to the loading phase of the experiment. This figure shows the effects of fluid perfusion on the overall longitudinal stress of the thin walled polymer tubes.

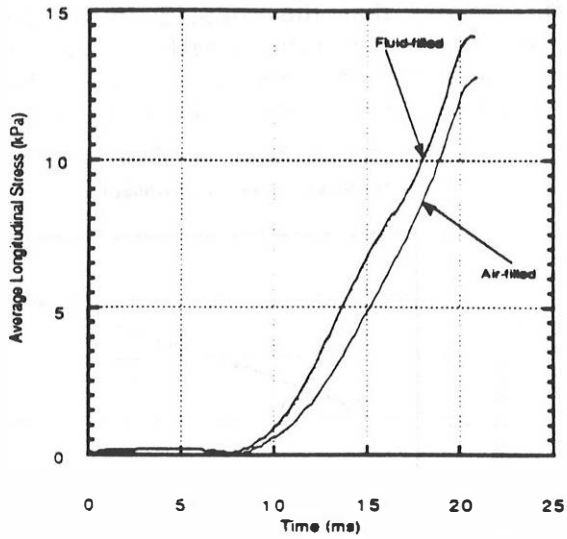

Figure 6 Comparison of Stress for Fluid and Air Filled Elastic Tubes

Figure 7 shows strain energy versus strain plots for the same experimental set of polymer tubes. Figure 7 shows a 17 percent increase in strain energy for the fluid versus air filled tube. This strain energy is the basis for modelling and comparison to existing models in the literature. This figure best illustrates the differences between the perfused and non-perfused cases.

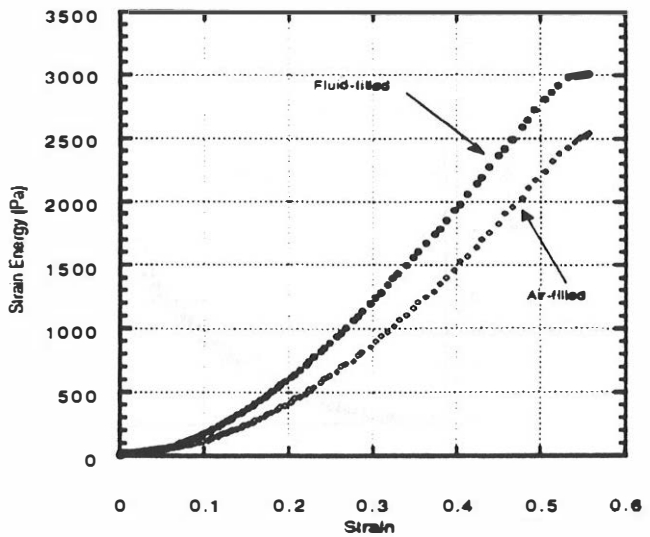

Figure 7 Comparison of Strain versus Strain Energy for Fluid and Air -filled Elastic Tubes

In addition to the experiments described above, a series of experiments have been done using various strain rates on air and fluid filled polymer tubes. These results are summarized in Figure 8. This figure reveals the relatively elastic nature of the air filled tube (insensitivity to strain rate) as compared with the more viscoelastic nature of the fluid filled tube. This viscoelastic behavior is due to the coupled fluid

and solid mechanics of this physical analog. In order to determine whether this viscoelasticity is due to the fluid viscosity or the fluid inertia, a series of experiments varying fluid viscosity have been performed. Figure 9 shows the results of experiments measuring a developed force increase of 27% from water to a pure glycerine mixture. This shows that the coupled fluid filled elastic tube behaves as a viscoelastic material although the tube itself is an elastic material. From our physical and numerical models we have determined that fluid viscosity and fluid inertia are relatively equal in their contributions to this effect.

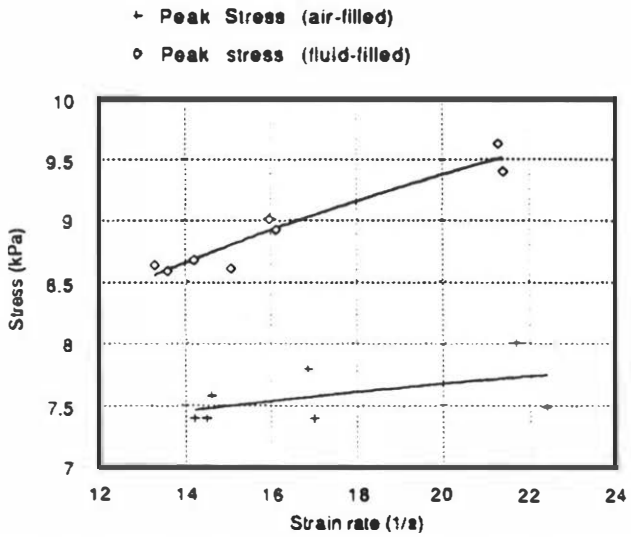

Figure 8 Comparison of Fluid and Air-filled Tubes for Various Strain Rates

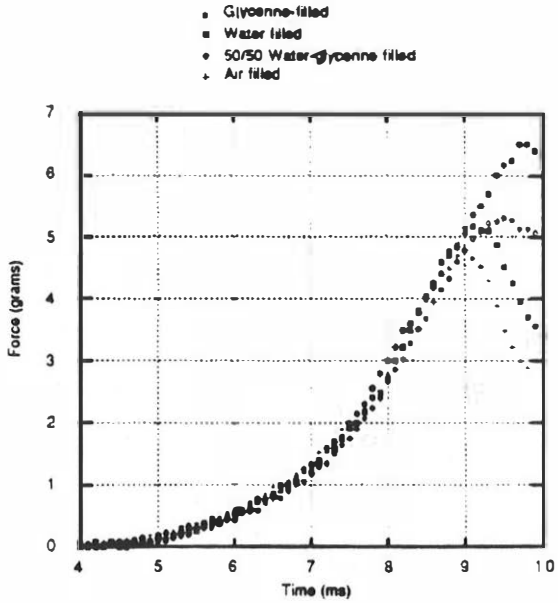

Figure 9 Comparison of Force for Different Viscous Fluid filled Tubes

To test the validity of this physical model, non-viable vessel specimes were tested analagously to the tubes. Non-viable blood vessels were utilized to eliminate the added effects of contractility. Results from non-viable blood vessels testing are shown in Figures 10 and 11. Figure 10 compares the blood vessels to a polymer tube analog, both traces have been taken to peak values in longitudinal stress. This shows the much stiffer nature of the blood vessel and more complex behavior than our simple analog. Figure 11 shows a comparison between a perfused and non-perfused non-

viable blood vesssel. This shows more sensitivity to the effects of fluid perfusion in the blood vessels. A very different character of material is revealed by these experiments. This is not an unexpected result since blood vessels are a composite material, however our physical analog shows similar trends when fluid perfusion is applied. This highlights the need for more accurate constitutive testing using perfused intact vessels to more accurately describe the physical situation involved in all trauma situations.

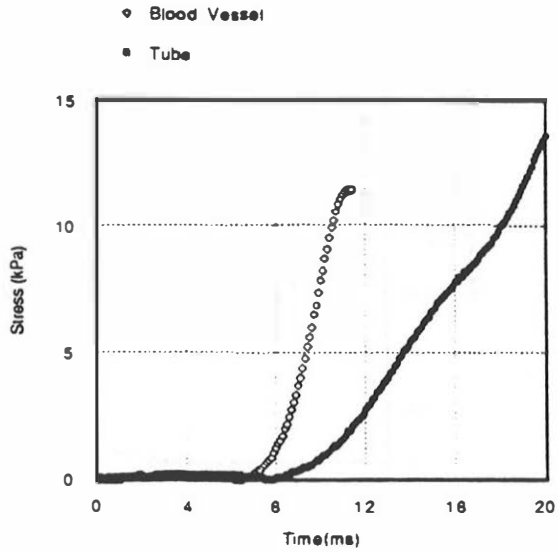

Figure 10 Comparison of Stress on Blood Vessel and Polymer Tube

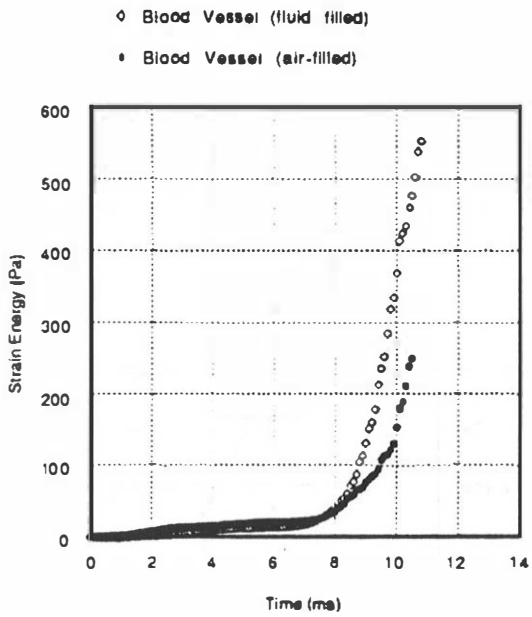

Figure 11 Comparison of Strain Energy for Fluid and Air-filled Blood Vessel

MODELLING

In order to determine more about the mechanical effects of perfusion on both vessels and tubes we need to model them. Our first model is a simple viscoelastic extension of the mechanics problem. The major drawbacks with this model are the fact that fluid conditions at the wall remain unknown. The other inherent problem is that an internal pressure function must be measured to complete the model. The viscoelastic formulations are very well suited to the uncertainties of blood vessel testing and are rather easy to calculate. A pressure function was assumed to be an

impulse in our first attempt at modelling with these viscoelastic formulations. This function will be measured directly in future experiments when the in line pressure transducer is in place. These results show good agreement with the data involving the wall mechanical properties.

Figure 12 shows the comparison of this model versus the strain energy of the thin walled perfused tube.

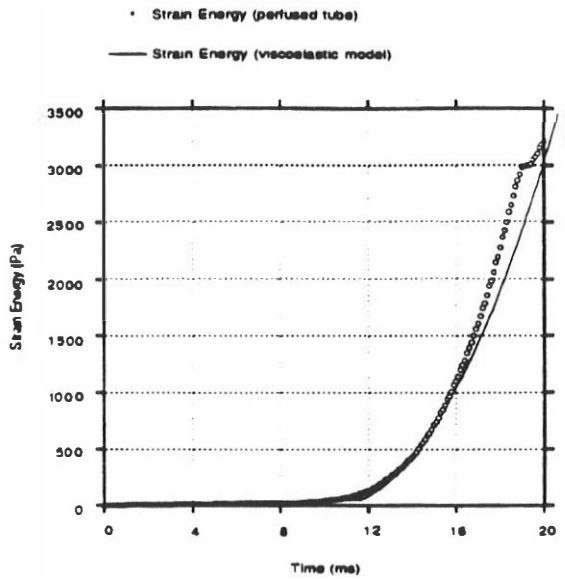

Figure 12 Comparison of Strain Energy for Perfused Tube and Viscoelastic Model

The model shows very good agreement in the shorter time scales. More detailed models are also being investigated at this time. The most promising is an extension of the analysis of Yang and Feng [27] to include fluid dynamic terms in their analysis of a the nonlinear elastic tube undergoing elongation. Figure 13 illustrates the results from this model and our extension which shows an increase in longitudinal stress for the fluid filled model similar to our experimental results. This model will be used to fully investigate the effects of fluid viscosity and fluid inertia as they contribute to these increased stresses.

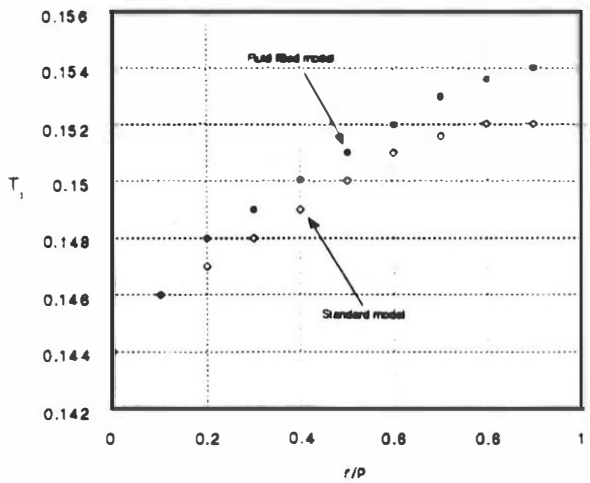

Figure 13 Comparison of Fluid filled and Standard Model for Nonlinear Elastic Tubes
where T_l is the longitudinal stress resultant
r/p is the nondimensional radius

CONCLUDING REMARKS

It is our desire to develop a range of neurovascular trauma indices. In vitro experiments confirm the vasoreactive response of isolated blood vessels to a single uniaxial high strain rate load. We can now fully develop dose-response relationships for the blood vessels in response to a pulse load and compare these values to those measured in the physical models of the brain undergoing inertial loading. With refinements, we can also study the mechanism of the injury and develop models for theraupetic intervention.

REFERENCES

1. Apter, Julia T. and Elsa Marquez : Correlation of Visco-Elastic Properties of Large Arteries with Macroscopic Structure, Circulation Research, Vol. 22: 393-404, 1968

2. Chuong, C. J. and Y. C. Fung: Three Dimensional Stress Distribution in Arteries, J. Biomechanical Engineering, Vol. 105: 268-274, 1983

3. Doyle, James and Philip Dobrin: Stress Gradients in the Walls of Large Arteries, J. Biomechanics, Vol. 16: 631-639, 1973

4. Eldevik, O. Petter, Kristian Kristiansen and Ansgar Torvik: Subarachnoid Hemorrhage and Cerebrovascular Spasm, J. Neurosurg, 55: 869-876,1981

5. Fenton, T. R., W. G. Gibson and J. R. Taylor: Stress Analysis of Vasoconstriction at Arterial Branch Sites, J. Biomechanics, Vol. 19(7): 501-509, 1986

6. Fung, Y. C.: Biomechanics: Mechanical Properties of Living Tissues, Prentice Hall, 1978

7. Fung, Y. C., K. Fronek and P. Patitucci: Pseudoelasticity of arteries and the Choice of its Mathematical Expression, Am. J. Physiol., 237(5): H620-H631, 1979

8. Gennarelli, T. A., L. E. Thibault, J. H. Adams, D. I. Graham, C.J. Thompson, R. P. Marcincin: Diffuse Axonal Injury and Traumatic Coma In the Primate, Annals of Neurology, Vol. 12, No. 6: 564-574, 1982

9. Gennarelli,T. A., L. E. Thibault, R. Tipperman, G. Tomei, R. Sergot, M. Brown, W. L. Maxwell, J. H. Adams, D. I. Graham, A. Irvine, L. M. Gennarelli, A. C. Duhaime, R. Boock, J. Greenberg: Axonal Injury in the Optic Nerve: A Model of Diffuse Axonal Injury in the Brain, J. of Neurosurgery, In Press

10. Johansson, Borje and Stefan Mellander: Static and Dynamic Components in the Myogenic Response to Passive Changes in Length as Revealed by Electrical and Mechanical Recordings from the Rat Portal Vein, Circulation Research, Vol. 36: 76-83, 1975

11. Johnston, I. H., J. A. Johnston and Bryan Jennett: Intracranial-Pressure Changes following Head Injury, The Lancet: 433-436, 1970

12. Kaplan, Barry et. al: Effects of Induced Hypotension during Experimental Vasospasm: A Neurological, Electrophysiological, and Pathological Analysis, Nuerosurgery, Vol. 19(1): 41-48, 1986

13. Lansman, Jeffry, Trevor Hallam and Timothy Rink: Single Stretch- Activated Ion Channels in Vascular Endothelial Cells as Mechanotransducers, Nature, Vol. 325: 811-813, 1987

14. Margulies, S.S., L. A. Thibault, T. A. Gennarelli: Physical Model Simulation of Brain Injury in the Primate, J. Biomechanics, in press

15. Miller, J. D. and J. D. Pickard: Intracranial Volume/Pressure Studies in Patients with Head Injury, Injury, Vol. 5(3): 265-268, 1974

16. Nagasawa, Shiro et. al: Mechanical Properties of Human Cerebral Arteries. Part 1: Effects of Age and Vascular Smooth Activation, Surg. Neurol., Vol.12: 297-304, 1979

17. Nagasawa, Shiro et. al: Mechanical Properties of Human Cerebral Arteries.Part 2: Vasospasm, Surg. Neurol., Vol. 14: 285-290, 1980

18. Nagasawa, Shiro et. al: Experimental Cerebral Vasospasm. Arterial Wall Mechanics and Connective Tissue Composition, Stroke, Vol. 13(5): 595-600, 1982

19. Nagasawa, Shiro et. al: Experimental Cerebral Vasospasm. Part 2: Contractility of Spastic Arterial Wall, Stroke, Vol. 14(4): 579-584,1983

20. Nagasawa, Shiro et. al: Biomechanical Study on Aging Changes and Vasospasm of Human Cerebral Arteries, Biorheology, Vol. 19: 481-489,1982

21. Ohta, Tomio and Maitland Baldwin: Experimental Mechanical Arterial Stimulation at the Circle of Willis,: 405-408,1967

22. Pfenninger E. G., A. Reith, D. Breitig, A. Grunert, F. W. Ahnefeld: Early Changes in Intracranial Pressure, Perfusion Pressure, and Blood Flow after Acute Head Injury. Part 1: An experimental study of the underlying pathophysiology, J. Neurosurg., Vol. 70: 774-779, 1989

23. Robert, M. and Leon Keer: An Elastic Circular Cylinder with Displacement Prescribed at the Ends-Axially Symmetric Case, Mech. Appl. Math., Vol 40(3): 339-363, 1987

24. Sparks, Harvey: Effect of Quick Stretch on Isolated Vascular Smooth Muscle, Suppl. Circulation Research, Vols. 14,15: I254-I260, 1964

25. Vaishnav, Ramesh, John Young and Dali Patel: Distribution of Stresses and of Strain Energy Density through the Wall Thickness in a Canine Aortic Segment, Circulation Research, Vol. 32: 577-583, 1973

26. Waters, Alan and David Harder: Altered Membrane Properties of Cerebral Vascular Smooth Muscle Following Subarachnoid Hemorrhage: An Electrophysiological Study, Stroke, Vol. 16(6): 990-997, 1985

27. Yang, W. H. and W. W. Feng: On Axisymmetrical Deformations of Nonlinear Membranes, J. of Applied Mechanics: 1002-1011, 1970

28. Young, W.C., Roark's Formulas for Stress and Strain, Sixth Ed., McGraw-Hill Book Co., 1989